DIRECTION DES ÉTUDES ET RECHERCHES

SERVICE APPLICATIONS DE L'ELECTRICITE ET ENVIRONNEMENT
DÉPARTEMENT LABORATOIRE NATIONAL D'HYDRAULIQUE

EDF
Electricité de France

Août 1996

DEUTSCH E.
MECHITOUA N.
MATTEI J.D.

SIMULATION D'ECOULEMENT FAIBLEMENT DEBITANT DANS LES PIQUAGES. COMPARAISON DES MODELES RIJ-EPSILON ET K-EPSILON

FLOW SIMULATION IN PIPING SYSTEM DEAD LEGS USING SECOND MOMENT, CLOSURE AND K-EPSILON MODEL

Pages : 12

96NB00180

Diffusion : J.-M. Lecœuvre
EDF-DER
Service IPN. Département PROVAL
1, avenue du Général-de-Gaulle
92141 Clamart Cedex

ISSN 1161-0611

SYNTHÈSE :

Cette note illustre les performances du modèle Rij-epsilon dans une application industrielle d'écoulement turbulent tridimensionnel : un piquage faiblement débitant. Les calculs sont menés avec le logiciel ESTET et comparent deux modèles de turbulence, le modèle de viscosité turbulente k-epsilon et le modèle de turbulence au second ordre Rij-epsilon. Trois maillages différents sont utilisés, un maillage grossier (100 000 noeuds), un maillage moyen (400 000 noeuds) et un maillage fin (1 500 000 noeuds). Les résultats du modèle Rij-epsilon sont meilleurs que ceux obtenus avec le k-epsilon à condition d'utiliser un maillage suffisamment fin. En effet, la pénétration de la vrille dans le piquage est alors mieux prédite.

Cette étude démontre la capacité du modèle Rij-Epsilon à être utilisé pour des études industrielles d'écoulements turbulents tridimensionnels. En effet, les calculs menés avec le modèle Rij-epsilon se sont déroulés aussi facilement qu'avec le modèle k-epsilon sans aucune précaution particulière. D'autre part le temps CPU utilisé avec le modèle Rij-epsilon est inférieur à 2 fois celui nécessaire au calcul k-ϵ.

EXECUTIVE SUMMARY :

This paper deals with an industrial application of second moment closure turbulence model in numerical simulation of 3D turbulent flows in piping system dead legs. Calculations performed with the 3D ESTET code are presented which contrast the performance of k-epsilon eddy viscosity model and second moment closure turbulence models. Coarse (100 000), medium (400 000) and fine (1 500 000) meshes were used. The second moment closure performs significantly better than eddy viscosity model and predicts with a good agreement the vortex penetration in dead legs provided to use sufficiently refined meshes. The results point out the necessity to be able to perform calculations using fine mesh before introducing refined physical models such as second moment closure turbulence model in a numerical code.

This study illustrates the ability of second moment closure turbulence model to simulate 3D turbulent industrial flows. Reynolds stress model computation does not require special care, the calculation is carried on as simply as the k-ϵ one. The CPU time needed is less than twice the CPU time needed using k-ϵ model.

Flow simulation in piping system dead legs using second moment closure and k-epsilon model

E. Deutsch N. Méchitoua, J.D. Mattéi
Laboratoire National d'Hydraulique / EDF
6, quai Watier, 78400 Chatou, France
Phone : 1 30.87.83.30
Fax : 1 30.87.72.53
Email : emmanuel.deutsch@der.edf.fr

1. INTRODUCTION

The "Laboratoire National d'Hydraulique" has been working since 1986 on the 3D ESTET code for simulating turbulent flows with complex physical models. The task of predicting these flows is made more difficult by the coupling of physical phenomena such as turbulence with 3D complex geometry. The 3D ESTET code provides an adequate framework for the implementation of second moment closure turbulence model to perform industrial calculations. This work presents numerical simulation of 3D turbulent flow at the junction between an auxiliary line and primary circuit of Pressurised Water Reactors. Hydraulic phenomenon is complex. There is a high Reynolds number flow in the main pipe (1 million) and a very small flow-rate in the auxiliary pipe referred to as "dead leg". Due to the shear at the junction, the flow is recirculating in the dead leg. Previous experiment (Robert, 1992) has shown that the symmetry of this recirculation with respect to the plane including the axes of two pipes may break down, then a swirling flow extends along the dead leg. A previous numerical study (Robert, Mattéi, 1990) with 3D ESTET code using k-epsilon turbulence model and coarse mesh failed to predict non-symmetrical flow and vortex penetration in the dead leg. Recent improvement in numerical techniques and computational performances allows to take into account larger mesh and to use more complex physical models like second moment closure turbulence model. The objective is to demonstrate the ability of second moment closure to predict this 3D industrial flows. To illustrate this point, calculations were carried on using k-epsilon and second moment closure turbulence models. Results was compared with flow pattern recently obtained by visualisation (Montanari and Deutsch, 1995).

2. MATHEMATICAL MODEL

The flows considered are, constant property, incompressible flows, governed by the mean flow equations :

2.1 Mass balance

$$\frac{\partial}{\partial x_j} U_j = 0 \tag{1}$$

where $U_j = \overline{u_j}$ (k=1,3) are the mean velocity components,

2.2 Momentum balance

$$\frac{\partial}{\partial t} U_i + \frac{\partial}{\partial x_j} U_i U_j = -\frac{1}{\rho}\frac{\partial P}{\partial x_i} + \frac{\partial \tau_{ij}}{\partial x_j} - \frac{\partial}{\partial x_j}\overline{u'_i u'_j} \tag{2}$$

where P is the mean pressure, ρ the density, τ_{ki} is the mean viscous stress tensor and $\overline{u'_i u'_j}$ the Reynolds stress.

The unknown Reynolds stresses in these equations are obtained either using the standard high Reynolds number k-ε model (Launder and Spalding (1974)) with the standard set of constants or the Reynolds stress transport equations model.

2.3 Reynolds stress transport equations

The Reynolds stress transport equations are expressed as :

$$\frac{\partial}{\partial t}\overline{u'_i u'_j} + U_k \frac{\partial}{\partial x_k}\overline{u'_i u'_j} = P_{ij} + d_{ij} + \phi_{ij} + \varepsilon_{ij} \tag{3}$$

where,

$$P_{ij} = -\overline{u'_i u'_k}\frac{\partial U_j}{\partial x_k} - \overline{u'_j u'_k}\frac{\partial U_i}{\partial x_k}, \tag{4}$$

is the rate of turbulence production by mean velocity gradient.

We follow the usual practice of modelling turbulent self-transport d_{ij} by gradient diffusion (Daly and Harlow, 1970).

$$d_{ij} = -\frac{\partial}{\partial x_k}\left(c_s \frac{k}{\varepsilon}\overline{u'_k u'_l}\frac{\partial}{\partial x_l}\overline{u'_i u'_j}\right) \tag{5}$$

ϕ_{ij} is the pressure-strain correlation. We adopt the simple model recommended by Launder (1989). This consists of a sum of the Rotta's return to isotropy term and the isotropisation of production model, $\phi_{ij} = \phi_{ij,1} + \phi_{ij,2}$,

$$\phi_{ij,1} = -c_1 \frac{\varepsilon}{k}\left(\overline{u'_i u'_j} - \frac{2}{3} k \delta_{ij}\right) \tag{6}$$

$$\phi_{ij,2} = -c_2 \frac{\varepsilon}{k}\left(P_{ij} - \frac{2}{3} P_{kk} \delta_{ij}\right) \tag{7}$$

Dissipation is assumed to be isotropic at high Reynolds number $\varepsilon_{ij} = -2/3\ \varepsilon\ \delta_{ij}$ where ε is obtained by the transport equation :

$$\frac{\partial}{\partial t}\varepsilon + U_j \frac{\partial}{\partial x_j}\varepsilon = -\frac{\partial}{\partial x_i}\left(C_\varepsilon \frac{k}{\varepsilon}\overline{u'_i u'_j}\frac{\partial}{\partial x_j}\varepsilon\right) - C_{\varepsilon 1}\frac{\varepsilon}{k}\frac{P_{ii}}{2} - C_{\varepsilon 2}\frac{\varepsilon}{k}\varepsilon \tag{8}$$

The following values of the constant are chosen :

C_s	C_1	C_2	C_ε	$C_{\varepsilon 1}$	$C_{\varepsilon 2}$
0.22	1.8	0.6	0.18	1.44	1.8

3. NUMERICAL METHOD.

The numerical techniques are based on finite difference and finite volume discretization and an accurate treatment of the fractional step method. The equations are discretized on a 3D semi-staggered grid, with pressure, Reynolds stress and epsilon at the centre of the control volume delimited by 8 velocity nodes. The mesh is single block structured.
The algorithm for the Navier Stokes solution relies on a segregated velocity-pressure formulation. Momentum, Reynolds stress and epsilon conservation equations are solved in the same way, using a quasi unsteady algorithm.
The advective terms are treated by a method of characteristics. The trajectory is approximated by a second order Runge Kutta scheme and a third order 3D Hermitian polynomial is used for interpolation. Diffusion with explicit and implicit source terms of dynamic variables (velocity, Reynolds stress and epsilon) is solved implicitly by a Gauss elimination method and alternating directions.
For the computations of the velocity components, a third step is required in order to prescribe the mass conservation, leading to a Poisson equation for the pressure increment.
In order to avoid non physical oscillations of the pressure field and the associated difficulties in obtaining a converged solution, a variant of the Rhie and Chow interpolation is used (Mechitoua et al., 1994).
A "local time step" technique can be used in order to rapidly reach the steady state for problems having zones at high velocity (main pipe) in the same time that zones at low velocity (auxiliary pipe).
For a steady flow computed as the limit of a transient, all variables are split in an explicit part and an increment. All increments tend towards zero with convergence in time; the splitting approximations have then little influence and the solution is independent of the chosen time step and of second order accuracy in space. This method has been extensively used for many years at the "Laboratoire National d'Hydraulique" for thermal-hydraulic computation with k-epsilon model and was extended to Reynolds stress transport equations (Bel Hassan, Simonin, 1993). The numerical difficulties of SMC is associated with replacing the stabilizing turbulent diffusion by divergence of Reynolds tensor. The stability of solution is obtained using procedure analogous to the apparent-diffusion technique proposed by Huang and Leschziner (1985). The Reynolds tensor increments appearing in the mean velocity equations are approximate by simple eddy-viscosity model. The source terms in the Reynolds stress equations were ordered so that the diagonal dominance of the coefficient matrix was maximised.

4. BOUNDARY CONDITIONS

Boundary conditions depend on the type of boundary which is to be dealt with.
At the inlet, the Dirichlet conditions are used on all the variables. Mean velocity, Reynolds stresses and dissipation were taken from a result of main pipe periodic computation. The standard pipe conditions are chosen for inlet conditions of auxiliary pipe. At the outlet, zero gradient conditions were applied for all transported variables. For walls a modelling based on a flat plate is used. The normal component of velocity satisfies an impermeability condition ($U_2=0$). Stress at the surface is defined as ρu_*^2, where u_*^2 is the friction velocity. For turbulent flows in pipes, the logarithmic velocity profile is well represented by

$$\frac{U_1}{u_*} = -\frac{1}{K}\ln\frac{u_* x_2}{\nu} + C$$

where K=0.41, C=0.52 and x_2 is the normal distance to the wall.

This law leads to determinate friction velocity using explicit value of tangent velocity U_1^n.
In a local frame related to the wall, the Reynolds stress conditions can be written as follows :

$$\overline{u'_1u'_2} = -\,u_*^2 \text{ (by definition)}\,,\ \overline{u'_1u'_3} = \overline{u'_2u'_3} = 0$$

$$\frac{\partial \overline{u'_1u'_1}}{\partial x_2} = \frac{\partial \overline{u'_2u'_2}}{\partial x_2} = \frac{\partial \overline{u'_3u'_3}}{\partial x_2} = 0$$

Neglecting viscous shear stress, and assuming that the turbulence production is mainly balanced by the viscous dissipation, the boundary condition on velocity gradient and dissipation is written :

$$\frac{\partial U}{\partial x_2} = \frac{u_*}{K\,x_2} \qquad \varepsilon = \frac{u_*^3}{K\,x_2}$$

5. EXPERIMENTAL CONDITIONS

The experimental system, described in detail by Montanari and Deutsch (1995), was used to obtain data on the various characteristics of the flow. A sketch of the mock-up is shown in figure 1.

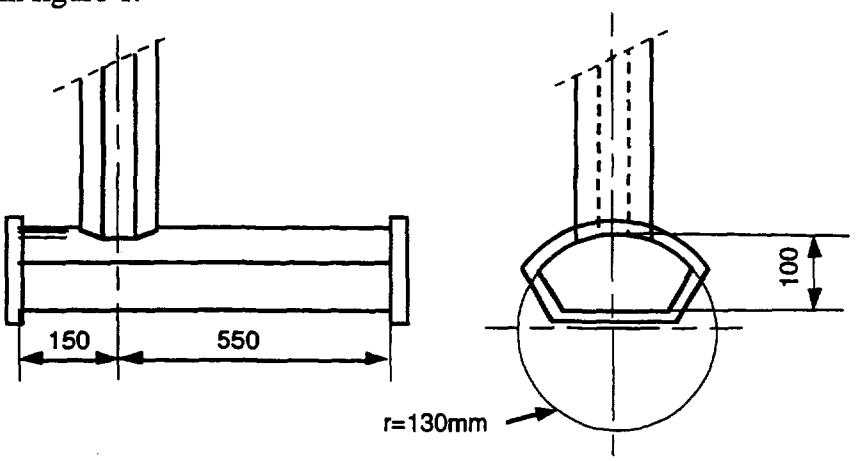

Figure 1 : Sketch of the mock-up.

The surface of the main pipe cross-section is S_m=1,3030.10^{-2}m^2 .
The dead leg diameter D is 100 mm. Its dimensionless length H/D is 20. The origin is located at the main pipe center. The pipe system dead leg is transparent, which enables visual observations of flow patterns. Light scattered perpendicular to a laser sheet was captured by a CCD camera. The flow pattern in the dead leg is determined by careful observation of the motion of tracer particles.
A set of three different injection velocities in the auxiliary pipe has been used.

main pipe velocity (m/s) Vm	9.2		
auxiliary pipe velocity (m/s) Va	0.092	0.046	0.023
Va/Vm	1 %	0.5 %	0.25 %

The Reynolds number based on the bulk velocity in the main pipe and the diameter of the dead leg is 895000 (ν=1.03 10^{-6} m^2/s).
The visual observations confirm previous experiment (Robert, 1992). Results for auxiliary pipe velocity Va = 0.023 is shown in figure 2. Due to the shear at the junction, the flow is recirculating in the dead leg (profile 3). The symmetry of this recirculation with respect to the plane including the axes of two pipes may break down (profile 2 and 4). Then a

corkscrew flow pattern shows up (profile 1 and 5). The hydraulic behaviour is the same for the three different injection velocities, but the length of vortex penetration depends on the injection velocity in the auxiliary pipe.

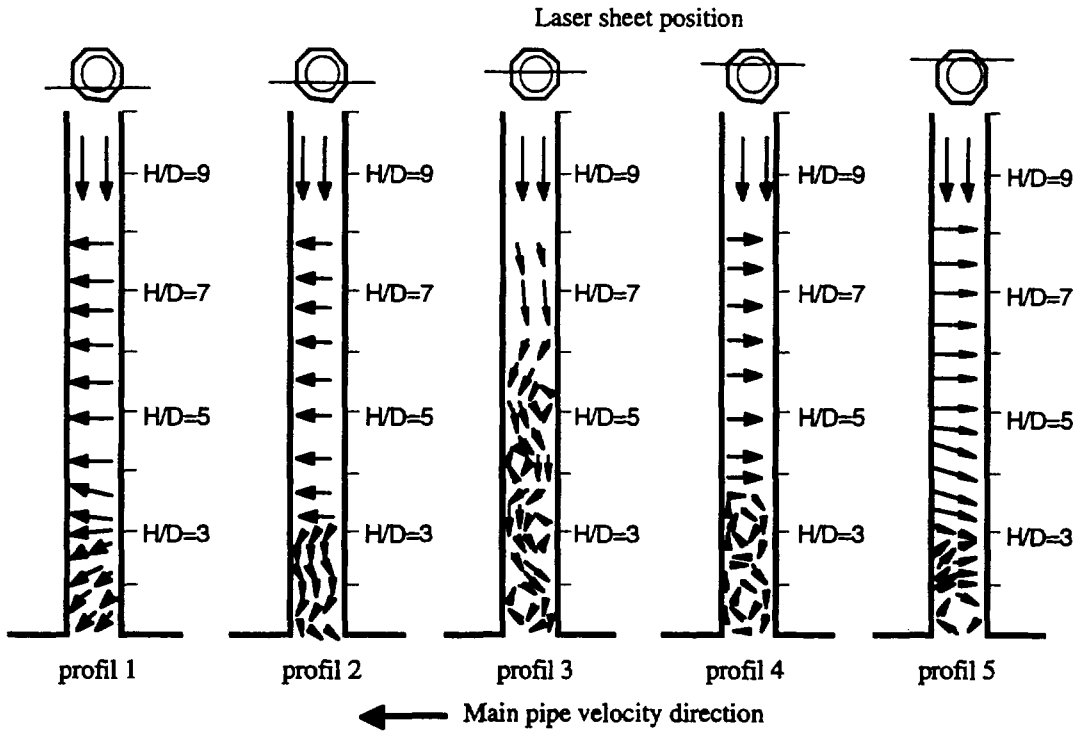

Figure 2 : Sketch of the flow obtained by visualisation (Va = 0.023).

6. NUMERICAL CALCULATIONS

In the present work, k-ε and second moment closure turbulence models have been used. A grid dependence study has been made with mesh of 35000, 150000, and 450000 internal nodes. Calculations are presented for the three different injection velocities in the auxiliary pipe.

Figure 3 displays the predicted vortex penetration using second moment closure, for a flowrate such that Va/Vm=0.25 %. Fluid particle trajectories and vertical velocity component in the auxiliary pipe illustrate a helicoidal flow pattern which develops as far as 9 diameters. The prediction of the velocity field is largely improved when increasing mesh size. Coarse mesh fails to predict the rotation of the flow. Both medium and fine meshes allow to predict the rotation, but the rotation power of the flow increases using the finest mesh.

Figure 4, shows the ability of standard k-epsilon model to predict non-symmetrical flow in the dead legs. Nevertheless the vortex penetration is not long enough, only as far as 6 diameters. The predictions using medium and fine mesh are very close. The finest mesh doesn't allow to improve the standard k-epsilon model prediction.

Figure 5 compares second moment closure and k-ε model predictions using fine mesh. Noticeable differences appear. Using Reynolds stress model (on the right), the flow obtained is very complex including many recirculations. It seems very similar to the

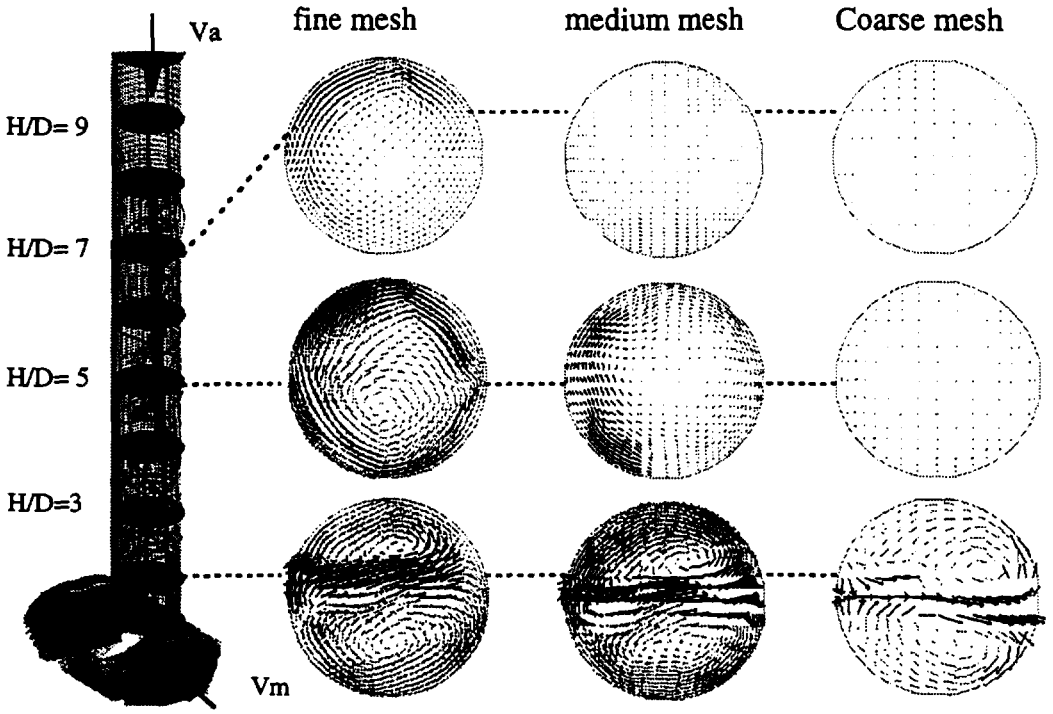

Figure 3 : Second moment closure prediction of vortex penetration in the dead leg : Va/Vm = 0.25 %. The positive vertical velocity component is displayed in Black and the negative in grey. Black trajectories represent fluid particles coming from the main pipe and grey trajectories represent the fluid particles coming from the top of the auxiliary pipe. Velocity vectors are plotted at three different sections of the auxiliary pipe H/D=2, 5 and 7 from the results of fine , medium and coarse mesh.

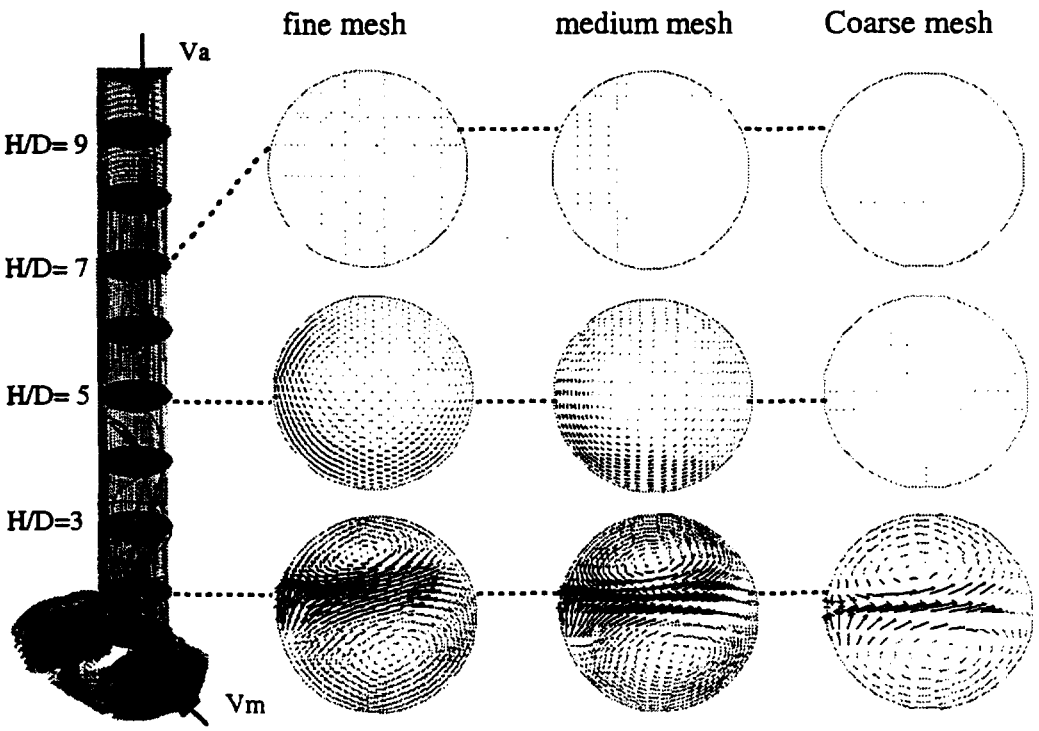

Figure 4 : k-ε prediction of vortex penetration in the dead leg: Va/Vm = 0.25 %.
The legend is the same as figure 2.

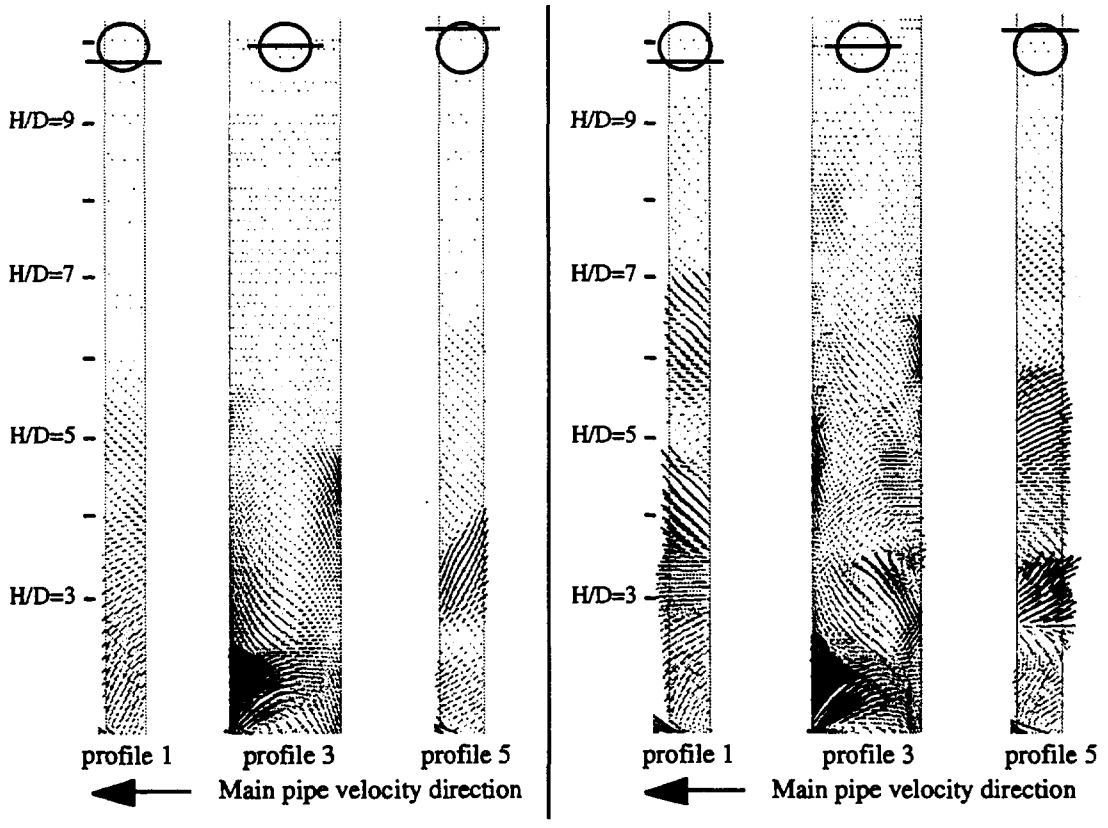

Figure 5 : predicted flow patterns, k-ε model (left) and second moment closure (right). Vector velocities with positive vertical component are displayed in Black and the negative in grey. On the top of the pipe each profile position is shown

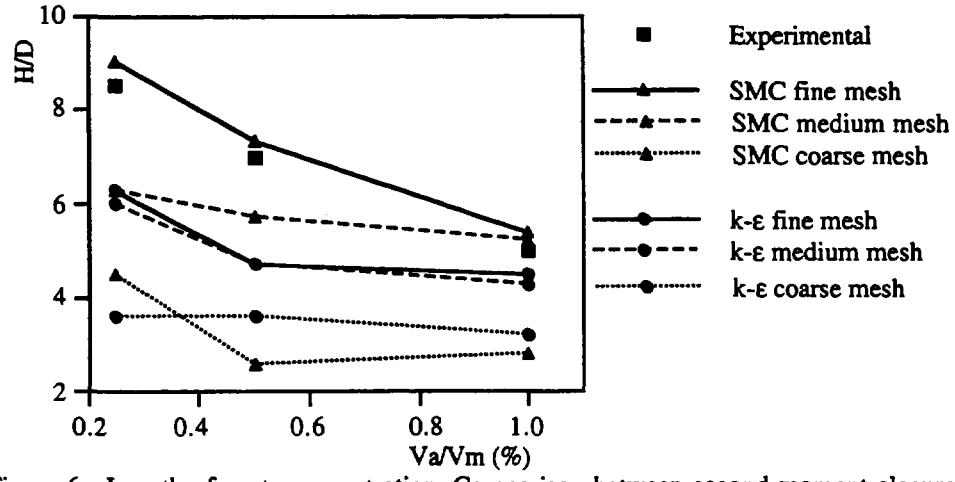

Figure 6 : Length of vortex penetration. Comparison between second moment closure (SMC) and k-ε model. Coarse, medium and fine mesh were used

visualised flow (figure 2). On the other hand, k-ε result (on the left) shows a different pattern. Due to the turbulent viscosity effect, the flow is more regular and small recirculations don't show up. The rotation velocity of the flow (profile 1 and 5) is clearly slower.
Figure 6 compares the length of vortex penetration prediction obtained by numerical simulation with experimental results. The results for three different flowrates are presented. Significant improvement is obtained when refining the mesh.
Second moment closure with fine mesh predicts with a very good agreement the vortex penetration in dead legs. The differences between medium and fine mesh illustrate the necessity to use very fine mesh with second moment closure. It might be necessary to perform a new simulation using finer mesh to achieve grid independence. The small difference between medium and fine mesh shows that k-ε model doesn't allow to predict a good vortex penetration even if more refined meshes are used.

CONCLUSION

Predictions of 3D turbulent flows in piping system dead legs has been done using k-ε and second moment closure. The second moment closure performs significantly better than eddy viscosity model and predicts with a good agreement the vortex penetration in dead legs provided to use sufficiently refined meshes. The results point out the necessity to be able to perform calculations using fine mesh before introducing refined physical models such as second moment closure turbulence model in a numerical code. This study illustrates the ability of second moment closure turbulence model to simulate 3D turbulent industrial flows. Reynolds stress model computation does not require special care, the calculation is carried on as simply as the k-ε one. The CPU time needed is less than twice the CPU time needed using k-ε model.

REFERENCES

Bel Hassan M., Simonin O., 1993, "Second-moment predictions of confined turbulent swirling flow", *Proc. 5thInternational Symposium on Refined Flow Modelling and Turbulence Measurements,* September 7-10, Paris, France.

Daly B. J., Harlow F. H., 1970, "Transport Equations in Turbulence", *Physics of fluids, Vol 13, n° 11, 2634-2649.*

Huang P. G., Leschziner M. A., 1985, "Stabilization of recirculating-flow computation performed with second-moment closure and third-order discretization", *Proc. 6th Symposium on Turbulent Shear Flows, 20.7 -20. 12.*

Launder B. E.,Spalding D. B., 1974, "The numerical computation of turbulent flows.", *Comp. Methods in Applied Mech and Eng., 3, 269-289.*

Launder B. E., 1989, "Second-moment closure : present...and future", *intl J. Heat Fluid Flow 10, 282-300.*

Mechitoua, N, J.D. Mattéi, D. Garréton, B. Chaumeton, 1994, "Three Dimensional Flow and Combustion Modelling of a Laboratory Gas Turbine Combustor", *International Symposium on Turbulence, Heat and Mass Transfer,* August 8-11, Lisbon, Portugal

Montanari, P., Deutsch E., 1995, "Thermohydraulique des piquages REP : Visualisation de l'écoulement à l'aide d'une tranche LASER.", *EDF report HE-44/95/036/A.*

Robert, M., 1992, "Corkscrew flow patern in piping system dead legs.", *NURETH-5,* September, Salt Lake City, USA.

Robert, M., Mattéi J. D., 1990, "Thermal hydraulic phenomena in a zero flowrate pipe connected to high flowrate, high temperature circuit Modelling.", *International Symposium on Engineering Turbulence Modelling and Measurements,* September 24-28, Dubrovnik, Yugoslavia.